The Effect of Natural Aging on Precipitation in Al-Mg-Si Alloys

F.A. Martinsen [a,*], M. Torsæter [a], F.J.H Ehlers [a], R. Holmestad [a]

[a] *Department of Physics, Norwegian University of Science and Technology, N-7491 Trondheim, Norway.*

Abstract

The effect of clustering during natural aging of three different Al-Mg-Si alloys with equal Mg/Si-ratios, but different Mg+Si contents has been systematically studied in the present paper. Hardness measurements were performed both during natural aging (NA) and after artificial aging (AA) preceded by various NA times. This revealed the existence of three different clustering processes: (i) An initial process causing a slight hardness increase during NA, while a strong hardness increase during subsequent AA. (ii) A second process causing a significant hardness increase during NA while a clear decrease in hardness after subsequent AA. (iii) A third process causing a hardness increase both during NA and after NA+AA. The processes (i) and (ii) are both finished within ~hours at room temperature, while process (iii) continues significantly longer (~ months). Since the latter process has a positive effect on alloy hardness, it eventually leads to a reversal of the so-called negative NA effect observed for alloys of high solute content. The variations in hardness were verified by investigating selected alloy conditions by transmission electron microscopy (TEM). The results established that measures like the precipitate number density, size and volume fraction vary according to the NA+AA hardness curves. Based on comparisons with previously published results, it is suggested that reaction (i) is due to Si-Si clustering, reaction (ii) Mg-Mg clustering and reaction (iii) Mg-Si clustering.

Key words: aluminium alloys, natural aging, artificial aging, hardness measurements, transmission electron microscopy (TEM)
PACS: 81.40.Cd, 61.46.Bc, 82.80.-d

1. Introduction

Al-Mg-Si (6xxx series) alloys are frequently used for industrial purposes due to the ease in which they can be formed, welded, anodized and painted. They are medium strength materials that can be hardened through artificial aging (AA) at elevated temperatures (150°C-200°C), leading to the formation of precipitate particles that impede dislocation motion. Since a large energetical barrier needs to be overcome to form the equilibrium precipitate phase, β-Mg_2Si [1] and the pure Si particles, the process goes through a number of metastable structures [2]:

$$\text{SSSS} \rightarrow \text{solute clusters} \rightarrow \text{GP zones} \rightarrow \beta'' \rightarrow \beta', U_1, U_2, \text{B}' \rightarrow \beta/\text{Si} \quad (1)$$

Detailed information on the structurally well-developed intermediate phases, starting from GP zones, can be found elsewhere [3,4] - but the exact nature of the solute clusters is still debated [5]. These form during the early stages of AA heat treatment, but they are also reported to appear upon so-called natural aging (NA) at room temperature [6]. These NA clusters are of the utmost importance - since they affect the kinetics of precipitate formation throughout the precipitation sequence. As they impose such strong effects, and since a short period of NA is industrially unavoidable due to difficulties in relocating huge amounts of material in short times, the phenomenon requires a detailed study.

* Corresponding author. Adress: Department of Physics, Norwegian University of Science and Technology, N-7491 Trondheim, Norway. Tel.: +47 48239236.
Email address: fredrikamartinsen@gmail.com (F.A. Martinsen).

Most interestingly, it has been observed by Røyset et. al. [7] that the effect of intermediate NA before AA heat treatment varies according to the total solute content of the alloy. In alloys of Mg+Si>1wt% a *negative NA effect* was observed, while alloys of Mg+Si<1wt% displayed a *positive NA effect* on alloy hardness after AA. Microstructural studies by TEM [8] revealed that the negative NA effect was related to a lowering in number density of hardening precipitates, while APT studies of Chang et al. [9] revealed that the positive NA effect relates to a boost in precipitate formation during AA.

The negative NA effect is so-far the most well-known, as it takes place in the dense, most commonly applied Al-Mg-Si alloys. A simple way to avoid their hardness decrease, resulting from intermediate NA, would lead to huge profits for the aluminum industry. Alloys could then be strengthened at low cost - and aluminum alloys would compete more strongly against other materials in a wide range of applications. The problem is, however, that the NA effect is caused by nanoscale solute clusters that are not straight-forward to investigate. Their very small size, together with their coherent growth with the surrounding Al lattice, make them unsuitable for investigation by standard microscopic methods [10,6]. As a result, our knowledge about the NA clustering is still insufficient - even if the subject has been the topic of several studies.

The first researchers that aimed to investigate the earliest stages of phase separation in Al-Mg-Si alloys were Kovacs et al. [11] in 1972. They showed through simple resistivity measurements and comparisons with available data on Al-Si alloys that Si-Si clustering aided by quenched in vacancies was likely to be the first step of the process. This suggestion was in 1990 supported by Dutta and Allen [12] who, through differential scanning calorimetry (DSC) studies, concluded upon the formation of Si-Si clusters in the early stages of NA. Later, in 1994, Edwards et. al. [13] showed through DSC studies that two processes took place in this early stage of NA. By atom probe field ion microscopy (APFIM) they found evidence that these two processes could be connected to the formation of separate Mg and Si clusters.

With the advent of the three dimensional atom probe (3DAP), more in-depth studies of cluster sizes and compositions could finally be made [6,14]. These revealed that in addition to the separate Mg-Mg and Si-Si clusters, Mg-Si co-clusters are forming upon long NA storage times or slightly higher aging temperatures. This was later verified by 3DAP studies by De Geuser et. al. [15] in 2006 and Torsæter et. al. [16] in 2010, where all three kinds of clusters were observed in both studies.

The previously reported studies add some pieces to the puzzle, but an explanation of *why* the positive and the negative NA effects take place is still far from being found. Results obtained in different groups are difficult to compare due to the extreme sensitivity of early-stage clustering to variations in heat treatment procedure, Mg/Si ratio, Mg+Si content and possible additions of other impurity elements. Consequently, we will in this work report a comprehensive study displaying exactly how variations in NA storage time affect the alloy microstructure after AA. This is investigated both by hardness measurements and transmission electron microscopy (TEM). The study involves alloys of different solute content (high, medium, low), but the alloy Mg/Si ratio is kept fixed for all three. Our results verify many of the hypothesis made by other researchers - but a novel key observation is made: the negative NA effect is reversed upon long NA storage times. This means that resources spent in quickly transferring large amounts of aluminum from one oven to another are in vain - as hardness would be gained by just introducing a delay in the production process allowing the alloy to rest at room temperature for about two months before artificial aging heat treatment. In addition, this observation provides information allowing for a physically sound description of the NA clustering process.

2. Experimental

Three industrial Al-Mg-Si alloys with equal Mg/Si ratios, but different solute content (Mg+Si), were investigated in the present work. Their nominal compositions are given in Table 1, where they are labeled according to their level of solute: HS = high solute content, MS = medium solute content and LS = low solute content. All three alloys are seen to contain similar amounts of iron and manganese.

Table 1
Content of alloying elements in the different alloys in wt.%

Alloy type	Label	Al	Mg	Si	Fe	Mn
LS	6060	98.93	0.37	0.45	0.2	0.05
MS	6005	98.511	0.555	0.718	0.2	0.016
HS	6181	98.05	0.75	0.95	0.2	0.05

The original samples were long extrusion made billets with either circular or rectangular shape and were received from Hydro Al. Samples were made by cutting out ~3x3 cm pieces of thickness < 3mm, and these were given a initial SHT of 540°C for one hour in a salt bath before be-

ing water quenched (WQ) to room temperature (RT). The samples were further divided into two groups, depending on whether or not they were going to be artificially aged. The first group of samples were only left for RT-storage and were regularly measured for hardness during the storage. The samples in the other group were left for various RT-storage times before they were subsequently artificially aged for 36 hours in an oil bath at 175° and then water quenched to RT. The samples were then further polished and measured for hardness. The temperatures in the oil and salt baths were measured to be within ±2° of the quoted value using a Digitron Instrumentation K-type thermocouple. The hardness measurements were carried out on a Matzuzawa-1S unit using a load of 1000 grams, 15 seconds loading time and a load speed of 100μm/second. The instrument was consistently manually calibrated each time it was being used in order to obtain comparable results. Two types of hardness measurements were made: ordinary measurements where the average over 10 indents results in a point on the hardness curve, and measurements denoted *continuous* - where the measurement value of each indent is plotted. The latter plots were made to map the very quick initial hardness changes for each alloy.

From the NA+AA hardness results, three samples from the HS alloy and two from the LS alloy were selected for investigations by TEM. Specimens were polished using a Stuers Kuth Rotor grinding device mounted with silicon carbide grinding paper, before they were electropolished using an electrolyte of one part nitric acid and two parts methanol. The electropolishing was carried out using a Stuers TenuPol-5 operated at 20 V with a light stop value of 120, a pump flow rate of 38 and with the electrolyte held between -20° and -30°C during polishing. The specimens were further investigated in a Philips CM30 TEM with a LaB_6 filament operated at 150 kV. Thickness measurements were performed using a Gatan model 601 parallel electron energy loss spectrometer (PEELS) equipped with an EL/P software. For each alloy condition, a series of ten TEM images (x 144000 magnification) were taken together with corresponding thickness measurements for the purpose of quantifying the average precipitate sizes and number densities. Pictures with x 491000 magnification were taken in order to calculate the average precipitate cross sectional areas. The reason for taking 10 images was to reduce the effects that possible inhomogeneities of precipitates would cause on the results.

3. Results

Natural aging: The hardness of the three alloys during natural aging can be seen in Figures 1a, 1c and 1e. The results extending over the whole interval of different NA times have datapoints representing the mean of ten indentations. Additional series are included for short NA times, denoted *continuous*, where one datapoint represents one indent with the hardness measurement machine.

The hardness of the HS alloy (Figure 1a) is seen to increase rapidly for short NA times before it gradually becomes proportional with the logarithm of time after about five hours. The hardness of the MS alloy (Figure 1c) is observed to increase slowly for short NA times, then increase rapidly between 30 min and 10 hours and furhter slowing down again after 10 hours. The LS alloy (1d) is observed to increase more or less proportionally with the logarithm of time during the entire investigated time interval with only a slight change in slope visible for short NA times.

Natural aging + subsequent artificial aging: The hardness variations of the three alloys as a function of NA time before the fixed AA heat treatment are shown in Figures 1b, 1d and 1f. The HS alloy (Figure 1b) is seen to decrease in hardness for NA storage times up to about five hours. For prolonged NA, the hardness is observed to increase, and this continues for all further NA times. The MS alloy (Figure 1d) is observed to increase in hardness for NA storage times up to 30 minutes. Further, the hardness decreases abruptly - before it stabilizes after about 10 hours NA. In this latter interval only a slight hardness increase is observed. The LS alloy (Figure 1f) is seen to increase in hardness with NA times up to two hours. Further, the alloy is observed to drop slightly in hardness, before it increases again upon prolonged intermediate NA times.

TEM-results: Based on the NA+AA curves (Figure 1b, 1d and 1f), three samples from the HS alloy and two from the LS alloy were selected for TEM analysis. The HS samples had been stored at RT for 18 seconds, 7 hours and 119 days before the fixed AA heat treatment, while the samples selected from the LS alloy had been naturally aged 18 seconds and 209 days before AA. It was found that all samples contained mainly the needle shaped β" phase, and only a few β' and B' precipitates were observed along grain boundaries. Representative TEM images for the LS alloy conditions are provided in Figure 2, and they show that the microstructure of the alloy becomes finer for prolonged intermediate NA times. For the HS alloy, rep-

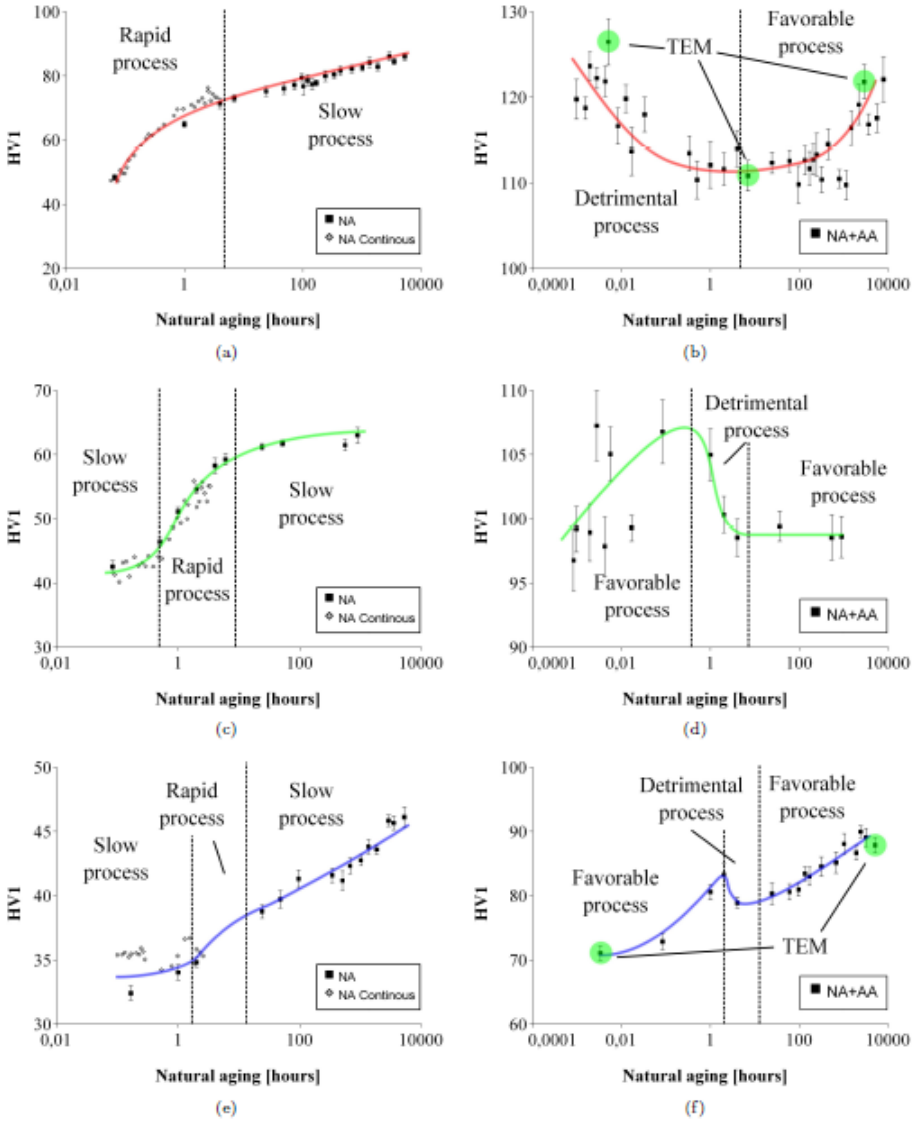

Fig. 1. The hardness results from the HS-alloys (a)-(b), MS-alloy (c)-(d) and LS alloy (e)-(f) plotted for both during NA (left) and after NA+AA (right). The colored lines are inserted as a guide for the eye, while the vertical dotted lines indicate where a change in slope of the curves are evident. These changes are seen to coincide for both NA and NA+AA hardness evolutions. This suggests that the effects appearing during NA are the ones causing the changes in the NA+AA curves. For figure (e) no evident changes are obserable, and the applied lines are drawn at equal times as in (f). The samples chosen for TEM-investigations are marked with dotted red rings.

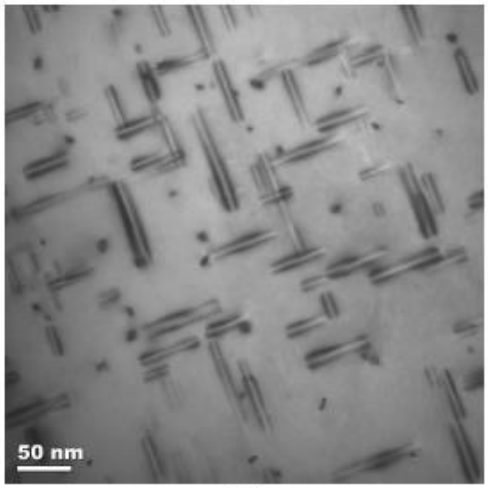

(a)

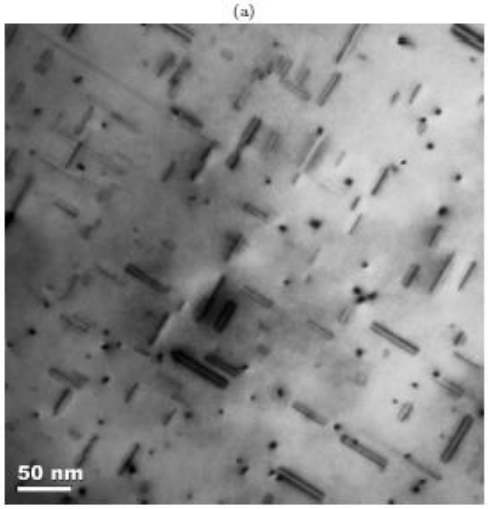

(b)

Fig. 2. TEM pictures of the LS alloy. Samples stored (a) 12 seconds and (b) 209 days at RT before AA. The sample in (a) can be observed to have a coarser microstructure than the one in (b).

resentative TEM images are given in Figure 3 - and they show that the microstructure qualitatively displays a clear *fine→coarse→fine* evolution for prolonged intermediate NA times.

A *quantification* of the microstructural details calculated based on TEM images can be seen in the plots in Figure 4. The volume fraction is here calculated by multiplying the other three quantities. As expected from qualitative observations, the precipitates of the HS alloy become larger and fewer if the sample is stored ∼hours compared to if it is stored for ∼seconds. For even longer NA storage times the precipitates in the HS alloy are observed to again become smaller and more numerous, but not as small and numerous as for the sample where NA storage was kept at a minimum. The volume fraction of precipitates for the various HS alloy conditions is seen to be almost equal for the samples stored 18 seconds and 7 hours, but it increases for the sample stored 119 days. For the LS alloy, the precipitates become smaller and more numerous for prolonged intermediate NA times - but the volume fraction is observed to be equal for the two investigated alloy conditions.

4. Discussion

4.1. *Three processes*

The hardness curves of the three alloys during NA (Figure 1a, 1c and 1e) can be directly compared with the hardness curves after NA+AA (Figure 1b, 1d and 1f). The TEM results obtained from chosen points of the latter curves (Figure 4) justify that the variations observed in the NA+AA curves actually mirror real microstructural changes in the alloys. The observation that there seems to be a correlation between the occurence of a process in both the NA and NA+AA curves justify the division of the curves into regions where different processes are believed to take place.

For the HS alloy a process is observed to happen between 0 and 5 hours of intermediate NA. This causes a rapid increase in the hardness during NA and a rapid decrease in hardness in the NA+AA curve. From TEM this process is found to lead to a coarsening of the microstructure. A second process is observed for prolonged NA times: the hardness during NA continues to increase, but the slope is less steep, and the NA+AA curve rises again. By TEM the process is found to lead to a finer microstructure.

For the MS alloy the clustering during NA can be divided into three parts: (i) A first reaction happening between 0 and 30 min of intermediate NA storage. It leads to a slight increase in hardness during NA, but causes a major increase in hardness after NA+AA. (ii) A second process happening between 30 minutes and 10 hours of intermediate NA storage. It leads to a large increase during NA, but a *de-*

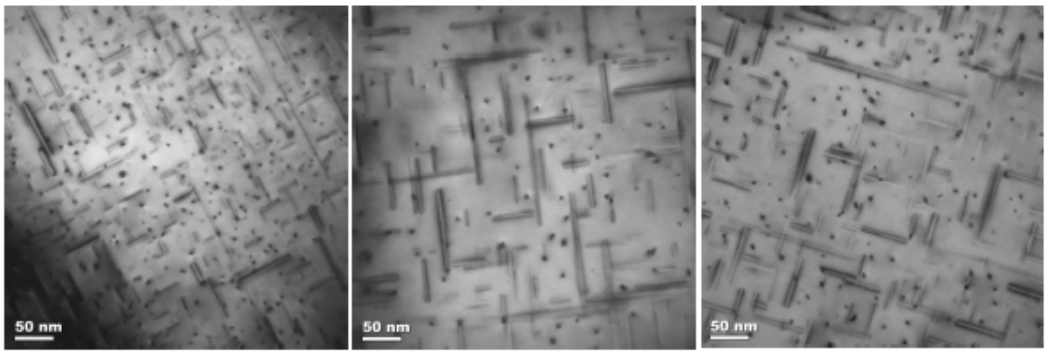

Fig. 3. TEM pictures of the HS alloy. Samples stored (a) 18 seconds, (b) 7 hours and (c) 119 days at RT before AA. The microstructure can be observed to follow a *Very fine→coarse→fine* pattern for prolonged intermediate NA times.

crease in the NA+AA curve. (iii) A third process observed to start after about 10 hours of intermediate NA and continue for all investigated prolonged NA times. It causes an increase in hardness during NA, but leads to a decrease in hardness for NA+AA.

For the LS alloy it is more difficult to divide the clustering processes into different parts. By interpreting the NA+AA hardness curve in the same way as for the MS alloy, however, one can explain some of the changes observed. The "bump" after 2-3 hours of intermediate NA storage can then be seen to correspond to the larger bump observed for the MS alloy. As there is much less solute in the LS alloy, the shift of the bump to longer NA storage times is as expected - since solute atoms statistically need to travel over longer distances to cluster in this alloy. The left part of the bump then indicates a fist process that lasts between 0 and 2 hours of intermediate NA, leading to no hardness increase during NA - but a visible increase in the NA+AA curve. The second process starts at the top of the bump, and ends at the bottom of it (after about 10 hours of intermediate NA). This process gives a visible hardness increase during NA and a visible *decrease* after NA+AA. Further, a thrid process takes place - starting after about 10 hours of NA and lasting throughout the investigated interval of intermediate NA storage times. It gives a hardness increase both during NA and after NA+AA.

As was acknowledged for the LS and MS curves, a striking resemblance is observed between the clustering behaviors in the various alloys. Assuming that the same "bump-interpretation" can be transferred to the HS alloy, the left part of the bump is here impossible to investigate. This is as expected, since this alloy is so packed with solute elements that statistically clustering can happen very quickly. The first measurements are thereby made at the top of the bump, meaning that the first process is already finished before measurements have started.

In summary, it is likely that three clustering processes can be distinguished for *all* Al-Mg-Si alloys: (A) Favorable process giving little hardness increase during NA, but providing an increase in hardness after NA+AA, (B) Detrimental process giving a rapid hardness increase during NA, but leading to a decrease in alloy hardness after NA+AA. (C) Favorable process giving a steady hardness increase during NA, and providing an increase in hardness after NA+AA. All three processes are observed to shift towards shorter NA times for increasing solute content, explaining why only the two last processes are observed for the HS alloy.

4.2. *A formation barrier*

Metastable phases appear earlier than the equilibrium phase in the precipitation sequence (1) because they are associated with a smaller formation barrier. This also applies to clusters, meaning that those associated with a small barrier will form before those associated with a larger one [17]. In literature it is reported that Si-Si and Mg-Mg clusters form first [14], and these are therefore likely to be associated with a lower formation barrier than the Mg-Si clusters that are reported to form later [6,18]. However, if an energy barrier needs to be surmounted to form the clusters, the same barrier must be surmounted to dissolve them. This stabilizes the clusters, and explains why only Mg-Si clus-

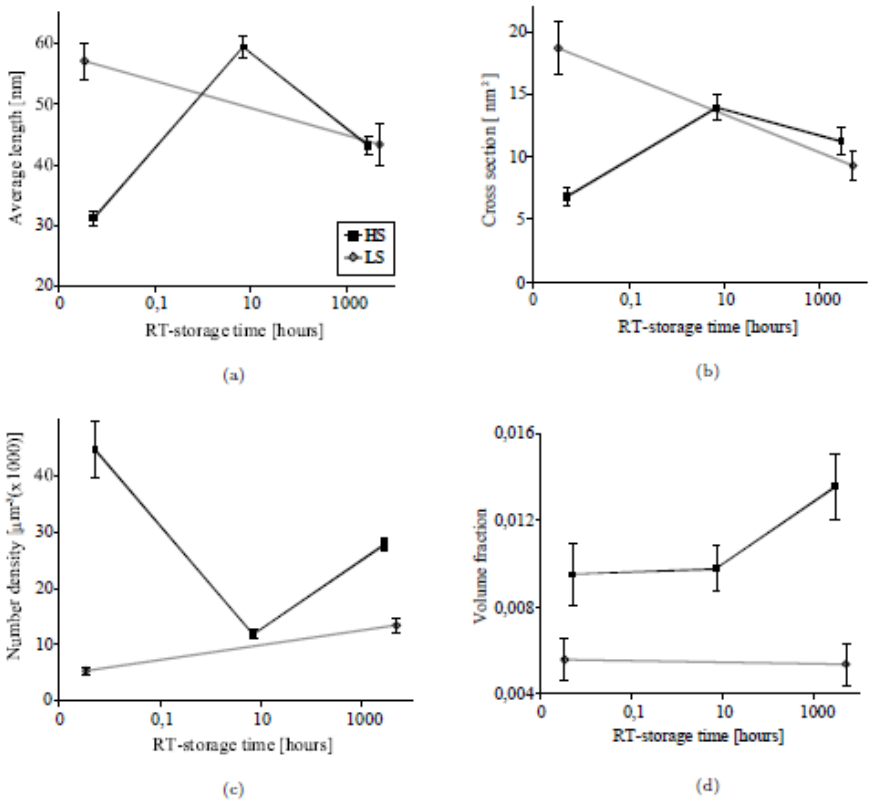

Fig. 4. An overview over the evolution in microstructure for the LS and the HS alloy as a function of NA time. (a) The variation in average precipitate length, (b) the variation in average cross section and (c) the variation in precipitate number density. The volume fraction variatioin displayed in (d) is found by multiplying the other three quantities.

ters survive heat treatment at 100°C [16]. It is also very likely that these slowly forming Mg-Si clusters enhance GP zone formation, as both structures are reported to have Mg/Si∼1 [6,16].

A recent study of Chang et al. [19] for the first time revealed three clustering peaks in DSC spectra, where the two first reactions happened very quickly - and the latter more gradually. This is in agreement with the three processes observed in our study, and by comparing to the previously reported sequence of clustering [14,15,13] it is likely that **process A** corresponds to Si-Si clustering, **process B** to Mg-Mg clustering and **process C** to Mg-Si clustering. This makes Mg-Mg clustering responsible for the detrimental effect of NA. The reversal of the negative effect can then be assumed to be related to the Mg-Si clustering. As this is slow and thereby barrier related, it forms more stable complexes - that are likely to dominate the alloy microstructure upon prolonged aging (by forcing less stable aggregations to give up solute atoms, and thereby growing on their expense). The reversal of the negative NA effect will thereby correspond to the point where the stable Mg-Si clusters outnumber their less stable competitors.

5. Conclusion

The effect of clustering during natural aging of three Al-Mg-Si alloys with equal Mg/Si-ratios, but different Mg+Si contents have been studied by hardness measurements and transmission electron microscopy (TEM). Based on the results, the following conclusions may be drawn:

- Clustering during NA of Al-Mg-Si alloys is found to happen through three different processes. These processes may be labeled A, B and C, and appear during NA in the same order as listed below:

  Process A: Found to cause a positive effect on hardness during NA and after NA+AA with unknown effect on the microstructure. The clustering is likely to be associated with a low formation barrier, as it happens quickly, and according to previously reported results on cluster compositions it is likely related to Si-Si clustering.

  Process B: Found to cause a major increase in hardness during NA, and a decrease in hardness after NA+AA. The process is observed to cause a major coarsening in microstructure after AA, and it is this that causes the lowering in strength of the material. The clustering is likely to be associated with a low formation barrier, as it happens quickly, and according to previously reported results on cluster compositions it is likely related to Mg-Mg clustering.

  Process C: Found to cause an increase in hardness both during NA and after NA+AA. As the clustering reaction is slow, it is likely to be associated with a relatively high energy barrier, causing the resulting clusters to become more stable than those formed in the quick processes A and B. The more stable product of the reaction is, however, likely to eventually dominate the microstructure, forcing less stable complexes to dissolve or transform into such phases. By comparing to previously reported results on cluster compositions, this reaction is likely to be related to Mg-Si clustering.

- A new precipitation sequence is suggested, adding the three above processes in an early part of the sequence. As the three clustering processes can overlap, the clustering reaction that at any stage dominates the alloy microstructure is written in boldface:

$$\begin{aligned} \text{SSSS} &\rightarrow \textbf{Si clusters} \rightarrow \text{Si clusters, } \textbf{Mg clusters} \\ &\rightarrow \text{Si clusters, Mg clusters, } \textbf{Mg-Si clusters} \\ &\rightarrow \text{GP zones} \rightarrow \beta'' \rightarrow \beta', U_1, U_2, \text{B}' \rightarrow \beta/\text{Si} \end{aligned} \quad (2)$$

- The precipitate types formed during AA are found to be independent of NA. For the investigated heat treatment of 1 hour SHT at 540°C and 36 hours at 175°C the resulting precipitate types are dominated by β''.

References

[1] M. H. Jacobs.
The structure of the metastable precipitates formed during ageing of an Al-Mg-Si alloy . *Philosophical Magazine*, 26:1–13, 1972.

[2] G.A.Edwards, K. Stiller, G.L Dunlop, and M.J Couper.
The Composition of Fine-Scale precipitates in Al-MgSi-Alloys. *Materials Science Forum*, 217-222:713–718, 1996.

[3] S.J. Andersen, C.D. Marioara, R. Vissers, M. Torsæter, R. Bjørge, F.J.H. Ehlers, and R. Holmestad.
The Dual Nature of Precipitates in Al-Mg-Si Alloys. *Materials Science Forum*, 638-642:390–395, 2009.

[4] R. Holmestad, C.D Marioara, F. Ehlers, M. Torsæter, R. Bjørge, J. Røyset, and S.J Andersen.
Precipitation in 6xxx aluminum alloys. *Proceedings of the 12th International Conference on Aluminium Alloys, Yokohama, Japan, September 5-9*, 1:30–39, 2010.

[5] John Banhart, Cynthia Sin Ting Chang, Zeqin Liang, Nelia Wanderka Matthew D. H. Lay, and Anita J. Hill.
Natural Aging in Al-Mg-Si Alloys - A Process of Unexpected Complexity. *Advanced Engineering Materials*, 12, 2010.

[6] M. Murayama and K. Hono.
Pre-Precipitate Clusters and Precipitation Process in Al-Mg-Si Alloys. *Acta Materiala*, 47:1537–1548, 1999.

[7] Jostein Røyset, Tore Stene, Jan Anders Sæter, and Oddvin Reiso.
The Effect on Intermediate Storage Temperature and Time on the Age Hardenable Response of Al-Mg-Si Alloys. *Materials Science Forum*, 519:239–244, 2006.

[8] C.D Marioara, S.J Andersen, J. Jansen, and H.W Zandbergen.
The influence of temperature and storage time at RT on nucleation of the β'' phase in a 6082 Al-Mg-Si alloy. *Acta Materialia*, 51:789–796, 2003.

[9] C.S.T.Chang, I. Wieler, N. Wanderka, and J. Banhart.
Positive effect of natural pre-aging on precipitation hardening in Al-0.44 at%Mg-0.38 at% Si alloy. *Ultramicroscopy*, 109:585–592, 2009.

[10] John Banhart, Cynthia Sin Ting Chang, Zeqin Liang, Nelia Wanderka Matthew D. H. Lay, and Anita J. Hill.
The Kinetics of Natural Ageing in 6000 Alloys - a Multi-method Approach. *Proceedings of the 12th International Conference on Aluminium Alloys, Yokohama, Japan, September 5-9*, 1:381–388, 2011.

[11] I. Kovacs, J. Lendvai, and E. Nagy.
The Mechanism of Clustering in Supersaturated Solid Solutions of Al-Mg_2Ai Alloys. *Acta Metallurgica*, 30:975–983, 1972.

[12] I. Dutta and S.M. Allen.
A clorimetric study of precipitation in comercial aluminium alloy 6061. *Journal of Materials Science Letters*, 10:323–326, 1991.

[13] G.A.Edwards, K. Stiller, and G.L Dunlop.
APFIM investigation of fine-scale precipitation in aluminium alloy 6061. *Applied Surface Science*, 76/77:219–225, 1994.

[14] M. Murayama, K. Hono, M. Saga, and M. Kikuchi.
Atom probe studies on early stages of precipitation in Al-Mg-Si alloys. *Materials Science and Engineering A*, 250:127–132, 1998.

[15] F. De Geuser, W. Lefebvre, and D. Blavette.
3D atom probe study of solute atoms clustering during naturaal aging and pre-aging of an Al-Mg-Si alloy. *Philosophical magazine Letters*, 86:227–234, 2006.

[16] Malin Torsæter, Williams Lefebvre, Sigmund Andersen, Calin D. Marioara, John C. Walmsley, and Randi Holmestad.
Clustering Behaviour in Al-Mg-Si Alloys Investigated by APT. *Proceedings of the 12th International Conference on Aluminium Alloys, Yokohama, Japan, September 5-9*, 1:1385–1390, 2010.

[17] D. A. Porter, K. E. Easterling, and M. Y. Sherif.
Phase Transformations in Metals and Alloys. CRC Press, 3th edition, 1961.

[18] A.K Gupta and D.J Lloyd.
Study of Precipitation Kinetics in a Super Purity Al-0.8 Pct Mg-0.9 Pct Si Alloy Using Differential Scanning Calorimetry. *Metallurgical and Materials Transactions A*, 30:879–884, 1999.

[19] C.S.T.Chang and J. Banhart.
Low-Temperature Differential Scanning Calorimetry of an Al-Mg-Si Alloy. *Metallurgical and Materials Transaction A*, 10, 2011.

[20] J. Banhart, M.D.H Lay, C.S.T Chang, and A.J Hill.
Kinetics of natural aging in Al-Mg-Si alloys studied by positron annihilation lifetime spectroscopy. *Physical Review B*, 83:014101, 1–13, 2011.